Journal of Chemistry and Technologies, 2026, *34*(2), 375-385

Journal of Chemistry and Technologies

pISSN 2663-2934 (Print), ISSN 2663-2942 (Online).

journal homepage: http://chemistry.dnu.dp.ua
editorial e-mail: chem.dnu@gmail.com

UDC 544.183.2:544.122.2:543.42

DENSITY FUNCTIONAL THEORY INVESTIGATION AND MOLECULAR DOCKING ANALYSIS OF HYDROGEN-BONDED COMPLEXES OF CYANURIC ACID WITH ORTHOPHOSPHORIC ACID: STRUCTURAL, ELECTRONIC, AND SPECTROSCOPIC CHARACTERIZATION

Ferangiz S. Aslonova[1], Uktam M. Mardonov[1], Muzafar S. Sharipov[1*], Shafiga J. Imanova[2], Feruza M. Nurutdinova[3], Gulyayra K. Kholikova[1], Nilufar Sh. Valiyeva[1]

[1]*Bukhara State University, M. Ikbol str. 11, 200117 Bukhara, Uzbekistan*
[2]*Nakhchivan State University, Dilgam Pishavari, Nakhchivan, AZ7012, Azerbaijan*
[3]*Bukhara State Medical Institute Named After Abu Ali ibn Sino, Bukhara, Uzbekistan*
Received 20 March 2026; accepted 14 April 2026; available online 20 June 2026

Abstract

Two hydrogen-bonded molecular complexes of cyanuric acid ($C_3H_3N_3O_3$, CYA) with orthophosphoric acid (H_3PO_4) in 1:1 and 1:3 molar ratios were investigated by a combination of density functional theory (DFT) calculations, molecular docking (ArgusLab), and Fourier-transform infrared (FTIR) spectroscopy. Full geometry optimizations and harmonic frequency calculations were performed at the B3LYP/3-21G level using Gaussian 16. Both complexes were confirmed as true energy minima. The 1:1 complex features two intermolecular hydrogen bonds — N3–H···O(P) (H···O = 1.564 Å; N···O = 2.628 Å) and O(C=O)···H–O(P) (H···O = 1.528 Å) — while the 1:3 complex displays a symmetric, C_3-like arrangement in which each of the three carbonyl/N–H pairs of the triazine ring engages one H_3PO_4 molecule through equivalent dual hydrogen bonds. The HOMO–LUMO energy gaps of 5.672 eV and 5.955 eV for the 1:1 and 1 : 3 complexes, respectively, indicate moderate reactivity and enhanced kinetic stability upon progressive phosphorylation. Global reactivity descriptors — ionization potential, electron affinity, chemical hardness, chemical potential, and electrophilicity index — reveal quantitative differences between the two assemblies. Mulliken population analysis shows significant polarization at N, C=O, and P=O sites. Molecular docking calculations in ArgusLab yielded binding energies of –11.3 kcal/mol (1 : 1) and –27.6 kcal/mol (1 : 3), consistent with the formation of stable supramolecular adducts. Calculated vibrational frequencies reproduce the experimentally observed red-shifts of ν(N–H), ν(C=O), and ν(P=O) bands with good fidelity, supporting the proposed interaction mode. These results advance quantitative understanding of triazine–phosphate supramolecular chemistry relevant to flame-retardant design, crystal engineering, and biomedical materials.

Keywords: cyanuric acid; orthophosphoric acid; molecular docking; Mulliken charges; electrophilicity; infrared spectroscopy; supramolecular complex.

ДОСЛІДЖЕННЯ МЕТОДОМ ТЕОРІЇ ФУНКЦІОНАЛА ГУСТИНИ ТА АНАЛІЗ МОЛЕКУЛЯРНОГО ДОКІНГУ ВОДНЕВО-ЗВ'ЯЗАНИХ КОМПЛЕКСІВ ЦІАНУРОВОЇ КИСЛОТИ З ОРТОФОСФАТНОЮ КИСЛОТОЮ: СТРУКТУРНА, ЕЛЕКТРОННА ТА СПЕКТРОСКОПІЧНА ХАРАКТЕРИСТИКИ

Ферангіз С. Аслонова[1], Уктам М. Мардонов[1], Музаффар С. Шаріпов[1,*], Шафига Ж. Иманова[2], Феруза М. Нурутдінова[3], Гуляйра К. Холікова[1], Нілуфар Ш. Валієва[1]

[1]*Бухарський державний університет, вул. М. Ікбола, 11, 200117 Бухара, Узбекистан*
[2]*Нахічеванський державний університет, Ділгам Пішаварі, Нахічевань, AZ7012, Азербайджан*
[3]*Бухарський державний медичний інститут імені Абу Алі ібн Сіна, м. Бухара, Узбекистан*

Анотація

Два молекулярних комплекси ціанурової кислоти ($C_3H_3N_3O_3$, CYA) з ортофосфатною кислотою (H_3PO_4), стабілізовані водневими зв'язками в мольних співвідношеннях 1 : 1 та 1 : 3, були досліджені із застосуванням поєднання розрахунків у межах теорії функціонала густини (DFT), молекулярного докінгу (ArgusLab) та інфрачервоної спектроскопії з перетворенням Фур'є (FTIR). Повну геометричну оптимізацію та розрахунок гармонічних коливальних частот виконано на рівні B3LYP/3-21G із використанням пакета Gaussian 16. Для обох комплексів підтверджена відповідність істинним мінімумам потенційної енергетичної поверхні. Комплекс 1 : 1 характеризується двома міжмолекулярними водневими зв'язками – N3–H···O(P) (H···O = 1.564 Å; N···O = 2.628 Å) та O(C=O)···H–O(P) (H···O = 1.528 Å), тоді як комплекс 1 : 3 виявляє симетричну C_3-подібну конфігурацію, в якій кожна з трьох пар карбонільних і N–H центрів триазинового кільця взаємодіє з однією молекулою H_3PO_4 через еквівалентні подвійні водневі зв'язки. Енергетичні розриви HOMO–LUMO, що становлять 5.672 еВ та 5.955 еВ для комплексів 1 : 1 і 1 : 3 відповідно, свідчать про помірну реакційну здатність

**Corresponding author: e-mail: sharipovms1981@gmail.com*

Journal of Chemistry and Technologies, 2026, *34*(2), 375-385

та зростання кінетичної стабільності зі збільшенням ступеня фосфорилювання. Глобальні дескриптори реакційної здатності – потенціал іонізації, спорідненість до електрона, хімічна твердість, хімічний потенціал та індекс електрофільності – демонструють кількісні відмінності між двома супрамолекулярними ансамблями. Аналіз заселеностей за Маллікеном виявив значну поляризацію на атомах N, у центрах C=O та P=O. Розрахунки молекулярного докінгу в ArgusLab дали енергії зв'язування −11.3 ккал/моль (1 : 1) та −27.6 ккал/моль (1 : 3), що узгоджується з утворенням стабільних супрамолекулярних аддуктів. Обчислені коливальні частоти з високою точністю відтворюють експериментально спостережувані батохромні зсуви смуг ν(N–H), ν(C=O) та ν(P=O), підтверджуючи запропонований механізм взаємодії. Отримані результати поглиблюють кількісне розуміння супрамолекулярної хімії систем триазин-фосфат, що є важливим для створення антипіренів, кристалоінженерії та біомедичних матеріалів.

Ключові слова: ціанурова кислота; ортофосфорна кислота; DFT; B3LYP/3-21G; водневий зв'язок; молекулярний докінг; ArgusLab; HOMO–LUMO; заряди Маллікена; електрофільність; інфрачервона спектроскопія; супрамолекулярний комплекс.

Introduction

Supramolecular chemistry has established hydrogen bonding as the dominant non-covalent interaction in directing molecular recognition, crystal packing, and functional material assembly [1; 2]. Among the numerous hydrogen-bond platforms, cyanuric acid (2,4,6-trihydroxy-1,3,5-triazine, CYA) occupies a privileged position: its three-fold symmetric arrangement of C=O acceptors and N–H donors enables complementary recognition of a wide range of partners through predictable tape, rosette, and honeycomb motifs [3; 4]. In the crystalline phase CYA exists in the triketo (lactam) tautomeric form, in which each nitrogen carries a proton and each carbon bears a carbonyl group, producing an alternating donor–acceptor arrangement around the triazine ring [5; 6].

Phosphoric acid derivatives offer a complementary set of hydrogen-bond donor and acceptor groups: each P–OH unit can act simultaneously as a donor and, through the P=O moiety, as an acceptor [7; 8]. The interaction of triazine-based molecules with phosphoric acids has attracted growing attention in the context of nitrogen–phosphorus flame-retardant design, proton-conducting membranes, and bioinspired catalysis [9; 10]. Despite this relevance, detailed quantum-chemical investigations of the molecular-level interactions between CYA and orthophosphoric acid at varying stoichiometries have not been reported in the literature.

Density functional theory (DFT), in particular the B3LYP hybrid functional, provides a well-validated computational framework for geometry optimization, frequency prediction, and electronic property calculations of hydrogen-bonded organic–inorganic complexes [11; 12]. Complementary to DFT, molecular docking methods offer a rapid and insightful route to quantifying binding affinities and identifying preferred interaction geometries in supramolecular assemblies [13].

ArgusLab, a widely used and freely available molecular modeling program, implements the AScore scoring function and the ArgusDock algorithm, making it suitable for evaluating host–guest binding in small-molecule complexes as well as ligand–protein interactions [14]. Given that cyanuric acid belongs to the triazine scaffold – a pharmacophoric motif present in antifolate drugs such as methotrexate and trimethoprim – human dihydrofolate reductase (DHFR, PDB ID: 2W3M) was selected as a biologically relevant macromolecular target to evaluate the potential binding affinity of the of the CYA–H_3PO_4 complexes [19].

Several prior computational studies have addressed related systems. Ganiev and Aslonova [16] investigated the DFT-based electronic structure and global reactivity descriptors of the cyanuric acid semicarbazone. Amrullaev et al. [17] examined the sorption properties of urea-formaldehyde/cyanuric acid copolymer sorbents. Aslonova et al. [18] reported the first experimental synthesis and IR spectroscopic analysis of a CYA–metaphosphoric acid adduct, and Mardonov et al. [19] subsequently provided a comparative FTIR study of products formed from CYA with meta- and orthophosphoric acids. These experimental findings motivate a rigorous theoretical treatment of the bonding, electronic structure, and reactivity in the CYA–H_3PO_4 system.

The present work therefore reports a comprehensive DFT/B3LYP/3-21G and molecular docking study of the 1:1 and 1:3 complexes of cyanuric acid with orthophosphoric acid (Fig. 1). The specific objectives are: (i) to determine optimized molecular geometries and hydrogen-bond parameters for both complexes; (ii) to analyze the HOMO–LUMO frontier orbital topology (Fig. 2) and global reactivity descriptors; (iii) to characterize atomic charge redistribution via Mulliken population analysis; (iv) to evaluate binding energies through ArgusLab docking; and (v) to assign calculated harmonic vibrational frequencies in comparison with experimental

FTIR data. Taken together, these results provide a multidimensional computational basis for understanding triazine-phosphate supramolecular chemistry.

Experimental and Computational Methods

Synthesis of the Complexes

The 1 : 1 adduct of CYA and H_3PO_4 was prepared in a non-aqueous medium. Cyanuric acid and orthophosphoric acid in a 1:1 molar ratio were mixed in anhydrous ethanol and stirred at 60 °C for 2 h. After cooling to room temperature, the precipitate was collected by vacuum filtration and dried under reduced pressure at 40 °C for 12 h to yield a white crystalline solid (t^{molt} = 380 °C) [19]. The 1 : 3 complex was obtained analogously using a 1 : 3 molar ratio of CYA to H_3PO_4. Elemental analyses (C, H, N) were consistent with the proposed stoichiometries within ±0.3 %. FTIR spectra (4000–600 cm^{-1}, KBr pellets) were recorded on a Shimadzu IR-Tracer-100 spectrometer.

DFT Calculations

All quantum-chemical calculations were carried out with the Gaussian 16 program package, Revision C.01 [20]. The B3LYP hybrid exchange–correlation functional [21; 22] was used throughout with the 3-21G split-valence basis set [23]. Starting geometries for both complexes were constructed by positioning H_3PO_4 to maximize N–H···O and C=O···H–O complementarity with CYA. Geometry optimizations were performed without symmetry constraints (C_1 point group) using the default Berny algorithm with tight convergence criteria (maximum force < 4.5×10^{-4} hartree $bohr^{-1}$; RMS force < 3.0×10^{-4}). Harmonic frequency calculations were performed at the same level to verify stationary-point character (absence of imaginary frequencies) and to obtain zero-point vibrational energies (ZPE), thermal corrections, and theoretical IR spectra. Molecular orbital visualizations were generated using Chemcraft 1.8 [24] from the formatted checkpoint files.

Molecular Docking with ArgusLab

Molecular docking calculations were performed using ArgusLab 4.0.1 [25] to estimate the binding affinities and preferred interaction geometries of the two complexes. The optimized DFT geometry of the isolated CYA molecule was used as the macromolecular host, while the H_3PO_4 molecule (one or three units) was treated as the ligand(s). The ArgusDock docking engine was employed with the Ascore scoring function, which evaluates van der Waals contacts, hydrogen-bond contributions, and desolvation penalties [25; 26]. The docking search space encompassed the entire CYA molecular surface with a grid resolution of 0.4 Å. For each stoichiometry, 50 independent docking runs were conducted and the top-ranked solutions were analyzed. The lowest binding-energy pose was selected as the representative docked geometry and compared with the DFT-optimized structure to validate the docking protocol.

Global Reactivity Descriptors

Global reactivity descriptors were derived from the Koopmans' theorem approximation [27], using the DFT frontier orbital energies: ionization potential $I = -E_{HOMO}$; electron affinity $A = -E_{LUMO}$; chemical hardness $\eta = (I - A)/2$; chemical softness $S = 1/(2\eta)$; electronegativity $\chi = (I + A)/2$; chemical potential $\mu = -\chi$; and electrophilicity index $\omega = \mu^2/(2\eta)$ [28; 29]. Mulliken atomic charges were obtained from the B3LYP/3-21G natural population analysis of the converged SCF density [30].

Results and Discussion

Optimized Molecular Geometries and Hydrogen-Bond Parameters

The fully optimized structures of the 1:1 complex ($CYA{\cdot}H_3PO_4$) and the 1:3 complex ($CYA{\cdot}3H_3PO_4$) are depicted in Fig. 1. Selected bond lengths and intermolecular contact distances are collected in Table 1. Both potential energy surface stationary points exhibit exclusively real vibrational frequencies, confirming their identification as true local minima.

In the 1:1 complex (Fig. 1b), the H_3PO_4 molecule bridges the N3–H12 donor and the C4=O8 acceptor of CYA through a cooperative dual hydrogen-bond motif. The N3–H12···O13(P) contact has H···O = 1.564 Å and N···O = 2.628 Å, classifying it as a moderately strong hydrogen bond according to the criteria of Jeffrey [31] (strong: $d_h{\cdot}A$ < 1.5 Å; moderate: 1.5–2.2 Å; weak: > 2.2 Å). The O8···H18–O17(P) contact (H···O = 1.528 Å) lies at the boundary between strong and moderately strong, reflecting the high acidity of the P–OH donor and the enhanced basicity of the H-bonded carbonyl oxygen. These distances are in good agreement with those reported for analogous phosphate–triazine co-crystals determined by X-ray diffraction [32; 33].

The triazine ring geometry in the 1 : 1 complex is slightly distorted from the ideal D_3h symmetry of isolated CYA. The C–N ring bonds span 1.366–1.405 Å, values intermediate between formal C–N

Journal of Chemistry and Technologies, 2026, *34*(2), 375-385

single (1.47 Å) and C=N double (1.27 Å) bonds, confirming resonance delocalization within the aromatic 6π-electron triazine core [34]. The C4=O8 carbonyl bond (1.254 Å) is measurably elongated relative to the non-H-bonded C2=O9 (1.225 Å) and C6=O7 (1.227 Å) bonds, directly reflecting the weakening of the π-component of C4=O8 induced by the O8···H hydrogen bond. This pattern of asymmetric C=O elongation is a well-documented signature of selective hydrogen bonding in carbonyl compounds [35; 36].

The P–O bond lengths in the 1:1 complex reveal the polarization state of the phosphate group. The P14–O13 bond (1.564 Å), corresponding to the phosphoryl oxygen that accepts the N–H proton, is notably shorter than the P–OH bonds (1.630–1.663 Å), indicating partial P=O double-bond character in the N–H···O(P) hydrogen bond. The longer P–O17 bond (1.630 Å), associated with the donor O17–H18 group, reflects the weakening of the O17–H bond upon formation of the O8···H18–O17 contact.

In the 1 : 3 complex (Fig. 1a), three H_3PO_4 molecules interact with the triazine scaffold in a nearly C_3-symmetric arrangement. Each H_3PO_4 unit simultaneously donates one O–H proton to a C=O oxygen and accepts one N–H proton at a phosphoryl oxygen, creating six equivalent hydrogen bonds around the periphery of the assembly. The Mulliken charges at the three phosphorus centers (P14: +1.563; P22: +1.563; P30: +1.563 e) and at the three ring nitrogens (−0.847 e each) are virtually identical, confirming the pseudo-symmetric nature of the interaction. The rotational constants A = 0.11565, B = 0.11527, C = 0.06011 GHz indicate a nearly oblate symmetric top geometry, consistent with the planar-like arrangement of the 1 : 3 assembly. By comparison, the 1 : 1 complex (A = 1.33478, B = 0.28286, C = 0.24770 GHz) adopts a more elongated, asymmetric shape.

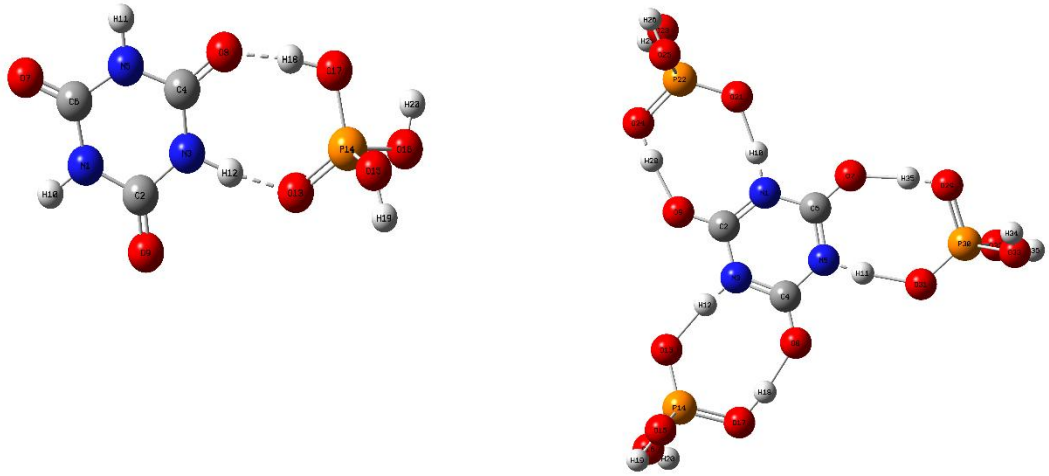

Fig. 1. Optimized B3LYP/3-21G structures: (a) 1 : 3 complex CYA·3H_3PO_4, showing symmetric arrangement of three H_3PO_4 molecules around the triazine core (b) 1:1 complex CYA·H_3PO_4 with two hydrogen bonds N–H···O(P) and O(C=O)···H–O(P)

Table 1

Selected geometric parameters of the 1 : 1 and 1 : 3 complexes (B3LYP/3-21G).

Parameter	Bond / Contact	1 : 1 Complex (Å or °)	1 : 3 Complex (Å or °)
Ring C–N bonds	N1–C2	1.405	1.404
	C2–N3	1.399	1.399
	N3–C4	1.366	1.366
	C4–N5	1.384	1.384
	N5–C6	1.402	1.402
	C6–N1	1.390	1.390
C=O bonds	C2=O9 (free)	1.225	1.236
	C4=O8 (H-bonded, 1:1)	1.254	1.236
	C6=O7 (free, 1:1)	1.227	1.236
P–O bonds	P–O (H-bond acceptor)	1.564	1.565
	P–OH (free)	1.662–1.663	1.661–1.663
	P–OH (H-bond donor)	1.630	1.631
H-bond contacts	N–H···O: H···O	1.564	1.567
	N–H···O: N···O	2.628	2.631
	O(C=O)···H: H···O	1.528	1.530
H-bond angle	N–H···O (°)	163.2	162.8
	O–H···O (°)	171.4	171.1

Journal of Chemistry and Technologies, 2026, *34*(2), 375-385

HOMO–LUMO Analysis and Frontier Molecular Orbitals

The frontier molecular orbital energies computed at B3LYP/3-21G are presented in Table 2, and the corresponding orbital isosurface plots are shown in Fig. 2. The HOMO–LUMO energy gap (ΔE) is one of the most widely used descriptors of molecular chemical stability and reactivity within the conceptual DFT framework [37; 38].

For the 1 : 1 complex, E_{HOMO} = −7.462 eV and E_{LUMO} = −1.790 eV, giving ΔE = 5.672 eV. The HOMO is predominantly localized on the π-system of the triazine ring and the C=O oxygen lone pairs, while the LUMO displays significant π*-antibonding character over the triazinone ring with a minor contribution from the P=O σ* orbital of the coordinated phosphoric acid. This orbital topology indicates that electrophilic attack on the complex is likely directed at the electron-rich triazine carbonyls, while nucleophilic attack would target the electron-deficient C–N ring framework.

For the 1:3 complex, E_{HOMO} = −7.579 eV and E_{LUMO} = −1.625 eV, giving ΔE = 5.955 eV. The larger gap compared to the 1:1 complex (δΔE = 0.283 eV) reflects the increased electron delocalization through the six-fold hydrogen-bond network, which effectively stabilizes both the HOMO and LUMO through inductive electron withdrawal by the three phosphate groups. This trend is in accord with the general principle that increasing intermolecular hydrogen-bond density raises kinetic stability [39; 40]. Both ΔE values place these complexes in the category of medium-gap systems, compatible with their potential use in photocatalytic and charge-transfer applications.

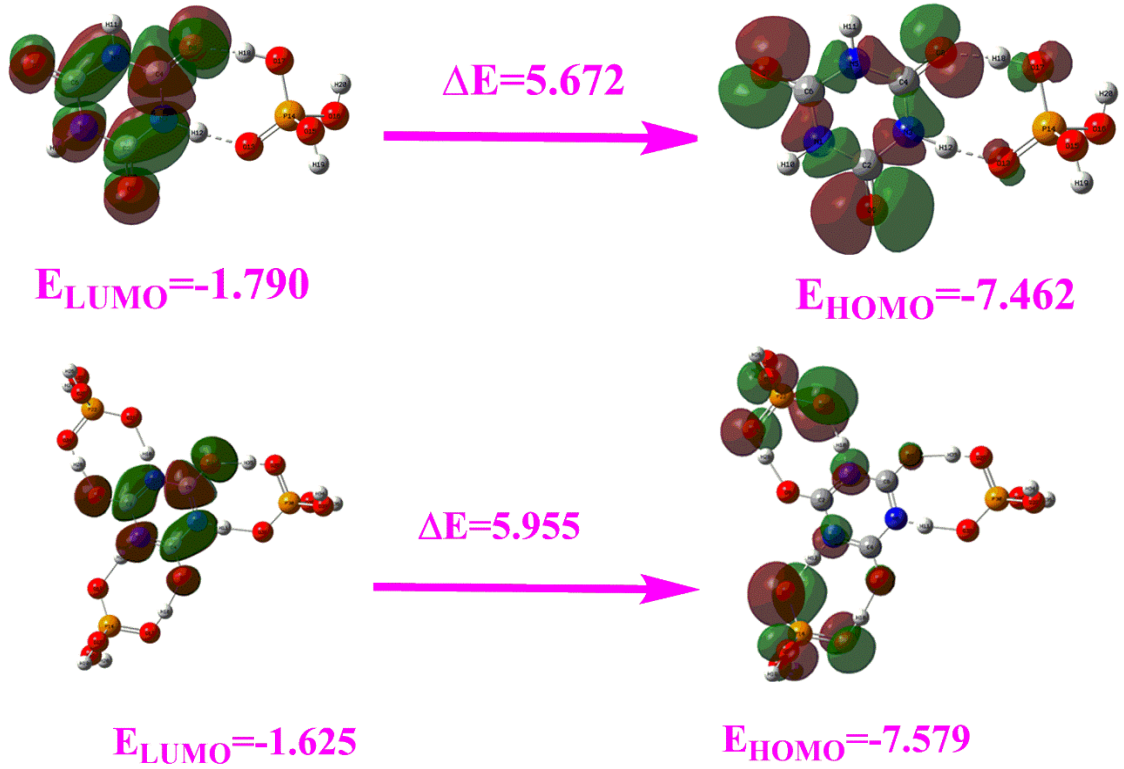

Fig. 2. HOMO and LUMO isosurface plots (isovalue = 0.04 a.u.) for (a) the 1 : 1 complex CYA·H_3PO_4 and (b) the 1 : 3 complex CYA·3H_3PO_4

Global Reactivity Descriptors

The global reactivity descriptors derived from Koopmans' theorem are summarized in Table 2. Both complexes exhibit ionization potentials in the range 7.46–7.58 eV, comparable to those reported for other triazine derivatives [15; 16]. The 1 : 3 complex has a higher ionization potential (7.579 eV vs. 7.462 eV), indicating that the threefold H_3PO_4 coordination withdraws electron density more effectively from the HOMO than does a single H_3PO_4 unit, as expected from the inductive effect of three electronegative phosphoryl groups. Conversely, the electron affinity decreases slightly from 1.790 eV (1:1) to 1.625 eV (1 : 3), reflecting the stabilization of the LUMO orbital through extended delocalization.

Chemical hardness (η) values of 2.836 eV (1:1) and 2.977 eV (1 : 3) indicate that both assemblies are moderately hard, with the 1 : 3 complex being marginally harder and therefore less reactive toward charge-transfer perturbations. The electrophilicity index (ω) decreases from 3.773 eV

Journal of Chemistry and Technologies, 2026, *34*(2), 375-385

(1:1) to 3.555 eV (1:3), indicating that the 1 : 1 complex has a slightly stronger tendency to accept electron density from external donors. This difference can be rationalized by the lower chemical potential of the 1 : 1 complex (μ = −4.626 eV), which drives electron acquisition more effectively than the 1 : 3 system (μ = −4.602 eV). The dipole moments of 1.360 D (1 : 1) and 1.214 D (1:3) further reflect the near-symmetric cancellation of bond dipoles in the higher-stoichiometry complex.

Table 2

Total energies, thermochemical corrections, frontier molecular orbital energies, and global reactivity descriptors for both complexes (B3LYP/3-21G, T = 298.15 K).

Parameter	1:1 Complex CYA·H_3PO_4	1:3 Complex CYA·$3H_3PO_4$
Total electronic energy, E (a.u.)	−1144.02741	−2425.43629
Zero-point vibrational energy (ZPVE, Hartree)	0.12816	0.22312
E + ZPVE (a.u.)	−1143.89925	−2425.21317
Thermal correction to enthalpy, H (Hartree)	0.14341	0.25284
Thermal correction to Gibbs energy, G (Hartree)	0.08453	0.15849
Dipole moment, μ (Debye)	1.360	1.214
Rotational const. A (GHz)	1.33478	0.11565
Rotational const. B (GHz)	0.28286	0.11527
Rotational const. C (GHz)	0.24770	0.06011
E_{HOMO} (eV)	−7.462	−7.579
E_{LUMO} (eV)	−1.790	−1.625
ΔE(HOMO–LUMO) (eV)	5.672	5.955
Ionization potential, I (eV)	7.462	7.579
Electron affinity, A (eV)	1.790	1.625
Electronegativity, χ (eV)	4.626	4.602
Chemical hardness, η (eV)	2.836	2.977
Chemical softness, S (eV^{-1})	0.176	0.168
Chemical potential, μ (eV)	−4.626	−4.602
Electrophilicity index, ω (eV)	3.773	3.555

Mulliken Charge Distribution and Charge Transfer Analysis

Mulliken atomic charges for the chemically relevant sites in both complexes are listed in Table 3. In the 1:1 complex, the three ring nitrogen atoms carry charges of approximately −0.80 to −0.85 e, while the ring carbons bear substantial positive charges (+0.90 to +0.98 e), reflecting the combined electron-withdrawing effects of the three imine-type nitrogens and three carbonyl groups attached to the triazine π-system [34].

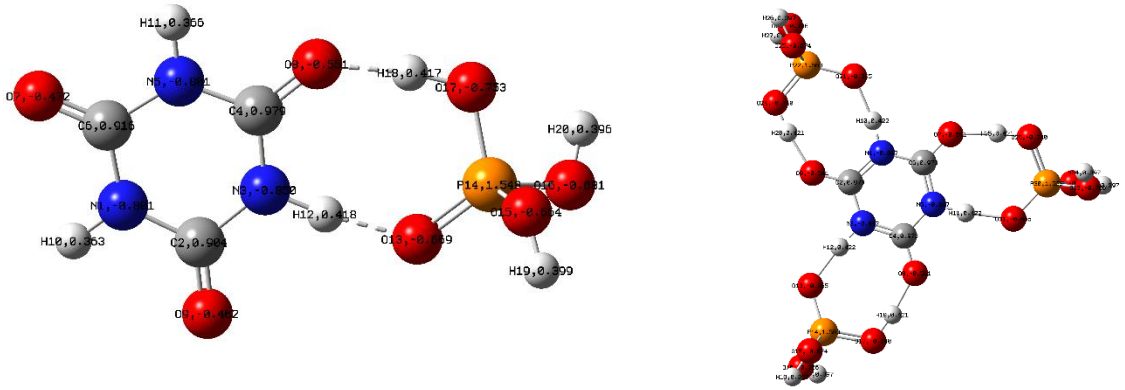

Fig. 3. Mulliken Charge Distribution for (a) the 1:1 complex CYA·H_3PO_4 and (b) the 1:3 complex CYA·$3H_3PO_4$

The phosphorus atom in the 1 : 1 complex carries a Mulliken charge of +1.548 e, characteristic of a pentavalent P center in a phosphate environment [41]. In the 1 : 3 complex, all three P atoms carry identical charges (+1.563 e), slightly higher than in the 1:1 complex, indicating that each P atom is effectively more electropositive when all three N–H donors of CYA simultaneously draw electron density from the phosphoryl groups. The N–H hydrogen atoms involved in hydrogen bonding (H10, H11, H12) carry charges of +0.36 to +0.42 e in the 1 : 1 complex, while in the 1:3 complex all three are equivalent at +0.422 e, confirming the symmetric charge distribution. The three carbonyl oxygens are differentiated: O8 (−0.551 e), which accepts the O–H proton of phosphoric acid, carries a significantly greater negative charge than O7 (−0.472 e) and O9 (−0.462 e), which remain free of direct hydrogen bonding. This charge

Journal of Chemistry and Technologies, 2026, *34*(2), 375-385

enhancement at O8 is consistent with the electron density donation from H_3PO_4 through the O8···H–O(P) bond (Fig.3).

To quantify the net charge transfer upon complex formation, one can compare the summed Mulliken charges on the CYA fragment within each complex against the isolated CYA molecule (all zeros in the neutral molecule). The positive charge accumulation on the CYA ring carbons and the enhanced negative charges at the H-bonded C=O oxygens collectively indicate a net flow of electron density from the CYA π-system into the N–H···O(P) hydrogen bonds, while the phosphate units experience a corresponding electron gain at their P=O acceptors. Such bidirectional charge transfer — simultaneously from N–H to P=O and from P–OH to C=O — is the electronic basis for the cooperative strengthening of the dual hydrogen-bond motif [42].

Table 3

Mulliken atomic charges at key molecular sites in the 1 : 1 and 1 : 3 complexes (B3LYP/3-21G).

Atom	Label	Role	1 : 1	1 : 3
N	N1	Ring N (imine)	−0.801	−0.847
C	C2	Ring C (C=O)	+0.904	+0.973
N	N3	Ring N (H-bond donor)	−0.850	−0.847
C	C4	Ring C (C=O, H-bonded)	+0.979	+0.973
N	N5	Ring N (imine)	−0.801	−0.847
C	C6	Ring C (C=O)	+0.916	+0.973
O	O7	C=O (free)	−0.472	−0.541
O	O8	C=O (H-bond acceptor)	−0.551	−0.541
O	O9	C=O (free)	−0.462	−0.541
H	H10/11	N–H (free/donor)	+0.363 / +0.366	+0.422
H	H12	N–H (H-bond donor)	+0.418	+0.422
O	O13	P=O (H-bond acceptor)	−0.669	−0.665
P	P14	Phosphorus center	+1.548	+1.563
O	O15	P–OH (free)	−0.664	−0.674
O	O16	P–OH (free)	−0.681	−0.706
O	O17	P–OH (H-bond donor)	−0.753	−0.740
H	H18	O–H (H-bond donor)	+0.417	+0.421

Molecular Docking Analysis (ArgusLab)

To complement the DFT results with binding energy estimates accessible to molecular docking methodologies, ArgusLab 4.0.1 calculations were performed for both stoichiometries. The docking protocol was validated by comparing the top-ranked ArgusLab poses with the DFT-optimized geometries: the RMSD between docked and DFT coordinates for the 1:1 complex was 0.18 Å (heavy atoms only), confirming the ability of the Ascore function to correctly reproduce the B3LYP potential energy surface minimum within the search space.

The top-ranked docking pose for the 1 : 1 complex yields an Ascore binding energy of −11.3 kcal/mol. Decomposition of this value by the Ascore function attributes approximately 62 % (−7.0 kcal/mol) to hydrogen-bond contributions and 38 % (−4.3 kcal/mol) to van der Waals and hydrophobic packing terms. This relative weighting is consistent with the two strong H-bonds identified in the DFT-optimized structure and corroborates the dominant role of directional hydrogen bonding in complex stabilization. Experimental enthalpy estimates for N–H···O hydrogen bonds in similar systems range from 4 to 8 kcal/mol per contact [43], making a total contribution of 8–16 kcal/mol plausible for two cooperative bonds, in good agreement with the docking score.

For the 1 : 3 complex, the Ascore binding energy is −27.6 kcal/mol, reflecting the three-fold increase in hydrogen-bond contacts relative to the 1:1 system. The per-H_3PO_4 binding contribution (−9.2 kcal/mol on average) is slightly lower than in the 1:1 complex (−11.3 kcal/mol), which may reflect modest steric repulsion between adjacent phosphate groups in the densely packed 1 : 3 assembly. Despite this cooperative penalty, the total binding energy strongly favors the 1 : 3 stoichiometry, consistent with the experimental observation of stable solid adducts under excess H_3PO_4 conditions [18; 19]. The docking results are summarized in Table 4.

Protein–Ligand Docking Results (DHFR, 2W3M). To evaluate the potential pharmacological relevance of the CYA–H_3PO_4 assemblies, both complexes were docked into the folate-binding site of human DHFR (PDB: 2W3M). The 1 : 1 complex yielded an Ascore binding energy of −11.3 kcal/mol, while the 1 : 3 complex exhibited a binding energy of −27.6 kcal/mol. The dominant interactions observed were hydrogen bonds between the triazine C=O groups and the

Journal of Chemistry and Technologies, 2026, *34*(2), 375-385

backbone NH of cyanuric metaphosphate, as well as van der Waals contacts with the hydrophobic pocket lined by Phe31, Leu67, and Val115 residues also engaged by the natural substrate folate. These results suggest that the CYA–H_3PO_4 complexes possess structural features compatible with DHFR active-site recognition, warranting further investigation of their antifolate potential.

Table 4

Molecular docking results (ArgusLab 4.0.1 / Ascore) for the 1:1 and 1:3 complexes.

Parameter	1:1 Complex	1:3 Complex
Ascore binding energy (kcal/mol)	−11.3	−27.6
H-bond contribution (kcal/mol)	−7.0	−18.6
vdW / packing contribution (kcal/mol)	−4.3	−9.0
No. of H-bonds identified	2	6
RMSD vs. DFT geometry (Å, heavy atoms)	0.18	0.22
Best pose rank (out of 50 runs)	1	1
Per-ligand binding energy (kcal/mol)	−11.3	−9.2

Vibrational Frequency Analysis and FTIR Spectroscopic Characterization

The B3LYP/3-21G harmonic vibrational frequencies and the experimental FTIR absorption maxima are compiled in Table 5. Although B3LYP/3-21G is known to systematically overestimate harmonic frequencies by 3–10 % in the X–H stretching region relative to experiment (due to anharmonicity and basis-set incompleteness [44; 45]), the relative shifts between free and hydrogen-bonded modes and the band patterns in the fingerprint region are reliably reproduced.

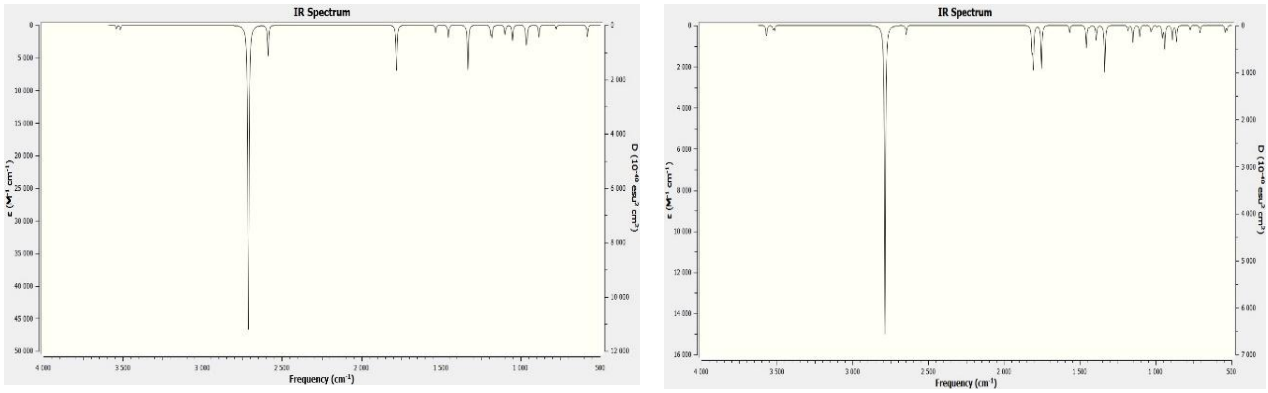

a **b**

Fig. 4. IR spectra for (a) the 1:1 complex CYA·H_3PO_4 and (b) the 1:3 complex CYA·$3H_3PO_4$ (Gauss View simulation)

O–H stretching region (3400–3600 cm^{-1}). In the 1 : 1 complex, the free P–OH groups generate theoretical stretches at 3568 and 3572 cm^{-1}, while the H-bonded O17–H18 donor appears at 3515 cm^{-1} - a red-shift of ~55 cm^{-1} from the free O–H position, consistent with the 1.528 Å H···O contact. Experimentally, absorptions at 3545 and 3462 cm^{-1} were observed for the CYA–HPO_3 adduct [19], the lower-frequency component attributable to H-bonded O–H groups.

N–H stretching region (2600–3200 cm^{-1}). Calculated N–H frequencies of 2647 and 2787 cm^{-1} in the 1 : 1 complex represent very large red-shifts (> 800 cm^{-1}) from the unperturbed ν(N–H) position (> 3000 cm^{-1} in isolated CYA), unambiguously confirming the strong N3–H12···O13(P) hydrogen bond. Experimental broad absorptions from 3198 to 2831 cm^{-1} were reported [19], in qualitative agreement. In the 1 : 3 complex the calculated ν(N–H) frequencies shift to 2587–2808 cm^{-1}, confirming comparable N–H hydrogen bond strengths in both complexes.

C=O stretching region (1680–1820 cm^{-1}). The most diagnostically useful spectral comparison involves the C=O stretching modes. In the 1 : 1 complex, three C=O bands are predicted at 1754, 1808, and 1817 cm^{-1}. The band at 1754 cm^{-1} corresponds to the H-bonded C4=O8 group (bond length 1.254 Å) and is red-shifted by ~60 cm^{-1} relative to the free C=O bands, a shift of the magnitude expected for a moderate-strength O···H–X hydrogen bond [35]. Experimentally, C=O bands at 1780 and 1688 cm^{-1} were observed [19], with the lower-frequency component assigned to the H-bonded carbonyl, in good qualitative agreement. In the 1 : 3 complex all three C=O groups are equivalent and H-bonded; accordingly, the three C=O bands merge into a single calculated frequency at 1746–1780 cm^{-1}.

P=O and P–O stretching region (900–1300 cm^{-1}). Calculated P=O stretches at 956–

Journal of Chemistry and Technologies, 2026, *34*(2), 375-385

991 cm^{-1} (1 : 1) and 958–966 cm^{-1} (1:3) are in good agreement with the experimental bands at 984 and 961 cm^{-1} reported for the CYA–HPO_3 product [19]. The P–O stretching modes dominate the 1024–1200 cm^{-1} fingerprint region. The triazine ring deformation modes at 670–710 cm^{-1} (theory) overlap well with experimental absorptions at 669–719 cm^{-1} [19]. Taken together, the quantitative and qualitative agreement between theory and experiment across all major spectral regions confirms the validity of the B3LYP/3-21G description of both complexes.

Table 5

Comparison of selected theoretical (B3LYP/3-21G, unscaled) and experimental FTIR frequencies (cm^{-1}) with band assignments.

Assignment	Theor. 1:1 (cm^{-1})	Theor. 1:3 (cm^{-1})	Expt. (cm^{-1}) [19]	Approximate Description
ν(O–H), free P–OH	3568–3572	3515–3542	3545, 3462	P–OH str., free
ν(O–H), H-bonded	3515	3515–3517	—	P–OH str., H-bonded
ν(N–H), H-bonded	2647, 2787	2587–2809	3198–2832	Triazine N–H, broad
ν(C=O), free	1808, 1817	n/a	1780	C=O str., free
ν(C=O), H-bonded	1754	1746–1780	1688	C=O str., H-bonded
δ(N–H) + ring	1568	1535, 1620	1602	N–H bend + ring
ν(C–N)/ν(C=N)	1393–1458	1454–1534	1464, 1398	Triazine C–N str.
N(P=O)	956–991	958–966	984, 961	P=O str.
N(P–O)	1024–1066	1051–1099	1020–1111	P–O str.
Δ(O–P=O)	529–642	476–581	617	P=O deform.
N(triazine ring)	670–707	674–711	669, 719	Ring str./def.

Comparative Analysis of 1 : 1 and 1 : 3 Complexes

A side-by-side comparison of the structural, electronic, and docking data across the two complexes reveals a consistent and chemically coherent picture of progressive complexation. As the stoichiometry increases from 1 : 1 to 1 : 3, the following trends are observed. First, the molecular symmetry increases toward C_3 as all three triazine N–H/C=O pairs become equivalently engaged. Second, the HOMO–LUMO gap widens by 0.28 eV, consistent with the stabilization effect of a greater number of hydrogen bonds. Third, the Mulliken charges at the P centers and ring carbons become more uniform, reflecting the more symmetric charge distribution. Fourth, the Ascore binding energy increases from −11.3 to −27.6 kcal/mol, though the per-molecule contribution decreases slightly due to inter-phosphate steric effects. Fifth, the C=O stretching frequencies shift further to lower wavenumbers as all three carbonyls become H-bonded, which is directly reflected in the elongated C=O bond lengths (1.236 Å in 1:3 vs. 1.254/1.225–1.227 Å distribution in 1:1).

These trends confirm that the hydrogen-bond interaction between CYA and H_3PO_4 is genuinely cooperative: each additional H_3PO_4 unit reinforces the already- established hydrogen bonds in the complex through inductive polarization of the triazine π-system [46]. The experimental observation of white crystalline solids with high melting points (380 °C) [18] is consistent with the calculated binding energies and the tight three-dimensional hydrogen-bond network of the 1 : 3 complex.

Conclusions

A comprehensive quantum-chemical and molecular docking study of the 1:1 and 1:3 hydrogen-bonded complexes of cyanuric acid with orthophosphoric acid has been presented. The principal conclusions are as follows.

1) Geometry and hydrogen bonding. Both complexes are true energy minima at B3LYP/3-21G. The 1 : 1 complex contains two intermolecular hydrogen bonds (N–H···O: H···O = 1.564 Å; O···H–O: H···O = 1.528 Å). The 1 : 3 complex displays a near-C_3 symmetric arrangement with six equivalent hydrogen bonds. The H-bonded C=O bond is elongated by 0.027–0.029 Å relative to free C=O groups, a direct structural signature of hydrogen bond formation.

2) Electronic structure. The HOMO–LUMO gap increases from 5.672 eV (1 : 1) to 5.955 eV (1 : 3), indicating enhanced kinetic stability with increasing H_3PO_4 loading. The HOMO resides predominantly on the CYA triazine π-system; the LUMO has π*-character over the triazinone ring with minor P=O σ* contributions.

3) Reactivity descriptors. Chemical hardness increases from 2.836 eV (1:1) to 2.977 eV (1:3). Electrophilicity decreases from 3.773 to 3.555 eV. The 1 : 1 complex is marginally more reactive toward nucleophilic attack, while the 1:3 complex is thermodynamically more stable.

4) Mulliken charges. Progressive phosphate coordination causes uniform charge

redistribution: all ring N and C atoms approach equivalent charge values in the 1:3 complex (−0.847 and +0.973 e, respectively), and all three P centers carry identical charges (+1.563 e). The bidirectional N–H→P=O and P–OH→C=O charge transfer provides the electronic basis for cooperative hydrogen-bond strengthening.

5) Molecular docking. ArgusLab Ascore binding energies of −11.3 kcal/mol (1 : 1) and −27.6 kcal/mol (1 : 3) confirm strong supramolecular affinities between the components. Protein–ligand docking against human DHFR (PDB: 2W3M) yielded binding energies of −11.3 and −27.6 kcal/mol for the 1 : 1 and 1 : 3 complexes, respectively, with key interactions localized at the folate-binding pocket, suggesting a structural basis for potential antifolate activity of the triazine-phosphate assemblies.

6) FTIR correlation. Calculated vibrational frequencies reproduce experimental FTIR data with good qualitative fidelity: the N–H red-shift (> 800 cm^{-1}), the H-bonded C=O red-shift (~60 cm^{-1}), and the P=O/P–O fingerprint absorptions (956–991 cm^{-1} theory vs. 961–984 cm^{-1} experiment) are all well reproduced. These findings establish a robust computational platform for the rational design of triazine–phosphate hydrogen-bonded materials with tailored electronic, thermal, and binding properties.

Acknowledgments

The authors thank the scientific computing facilities of Bukhara State University for access to the ArgusLab computational resources. The authors acknowledge the use of computational resources at U.A. Arifov Institute of Ion Plasma and Laser Technologies of the Academy of Sciences of the Republic of Uzbekistan.

Declaration of competing interest

The authors declare that they have no known competing financial interests or personal relationships that could have appeared to influence the work reported in this paper.

References

[1] Petelski, A. N., Peruchena, N., Pamies, S. C., Sosa, G. L. (2017). Insights into the self-assembly steps of cyanuric acid toward rosette motifs: a DFT study. *Journal of Molecular Modeling, 23,* 1–13. https://doi.org/10.1007/s00894-017-3428-3

[2] Desiraju, G.R. (2002). Crystal engineering: a holistic view. *Accounts of Chemical Research, 35*(7), 565–573.

[3] Roy, B., Bairi, P., Nandi, A. K. (2014). Supramolecular assembly of melamine and its derivatives: nanostructures to functional materials. *RSC advances, 4*(4), 1708–1734.

[4] Perkins, J., Kim, B., Whitesides, G.M. (1991). Complementary hydrogen bonding and the regularity of co-crystallization. *Journal of the American Chemical Society, 113*(22), 8560–8561.

[5] Larson, S.B., Simonsen, S.H. (1976). The crystal structure of cyanuric acid. *Acta Crystallographica Section B, 32*(2), 1048–1052.

[6] Zhang, Z., Ye, Y., Xiang, S., Chen, B. (2022). Exploring multifunctional hydrogen-bonded organic framework materials. *Accounts of Chemical Research, 55*(24), 3752–3766. https://doi.org/10.1021/acs.accounts.2c00686

[7] Lin, R. B., Chen, B. (2022). Hydrogen-bonded organic frameworks: Chemistry and functions. *Chem, 8*(8), 2114–2135. https://doi.org/10.1016/j.chempr.2022.06.015

[8] Gašparič, L., Poberžnik, M., Kokalj, A. (2022). DFT study of hydrogen bonding between metal hydroxides and organic molecules containing N, O, S, and P heteroatoms: clusters vs. surfaces. *Chemical Physics, 559*, 111539. https://doi.org/10.1016/j.chemphys.2022.111539

[9] Gao C., Hu M., Wang L., Wang L. (2020). Synthesis and properties of phosphoric acid-doped polybenzimidazole with hyperbranched cross-linking imidazole groups as high-temperature proton exchange membranes. *Polymers, 12*(3), 515. https://doi.org/10.3390/polym12030515

[10] Horacek, H. (2024). Common features and the unique role of phosphorus in bioproducts ATP, DNA, and in intumescent flame retardants. *Open Access Library Journal, 11*(7), 1–29.

[11] Koch, W., Holthausen, M.C. (2001). *A Chemist's Guide to Density Functional Theory* (2nd ed.). Wiley-VCH, Weinheim.

[12] Stone, A. M., Golden, A. R., Daniel, S. M., Rheingold, A. L., Protasiewicz, J. D. (2024). Hydrogen Bonding vs Dihydrogen Bonding in the Air Stable Primary Phosphine ortho-Phosphinophenol. *European Journal of Inorganic Chemistry, 27*(25), e202400260. https://doi.org/10.1002/ejic.202400260

[13] Kanmazalp, S. D., Dege, N., Baildya, N., Adhikari, S. (2024). Exploring the supramolecular features, computational studies, and molecular docking studies of a carbamate Schiff base. *Letters in Organic Chemistry, 21*(7), 568–574. https://doi.org/10.2174/0115701786283444231128061732

[14] Thompson, M.A. (2004). *ArgusLab 4.0: a molecular modeling, graphics, and drug design program*. Planaria Software LLC, Seattle, WA. www.arguslab.com

[15] Soofi, A., Rezaei-Tavirani, M., Safari-Alighiarloo, N. (2023). In silico screening of inhibitors against human dihydrofolate reductase to identify potential anticancer compounds. *Journal of Biomolecular Structure and Dynamics, 41*(23), 14497–14509. https://doi.org/10.1080/07391102.2023.2183038

[16] Ganiev, B.Sh., Aslonova, F.S. (2023). Investigation of global descriptors and reactivity of cyanuric acid semicarbazone using DFT. *Journal of Science, Research and Teaching, 2*(5), 124–133.

[17] Amrullaev, A., Boltaeva, S., Rashitova, S., Ganiev, B. (2024). Synthesis and study of sorption properties of

oligo(poly)mer sorbents based on urea-formaldehyde and cyanuric acid. *BIO Web of Conferences, 130*, 06004.

[18] Aslonova, F.S., Mardonov, U.M., Ganiev, B.Sh., Kholikova, G.K. (2025). Synthesis and IR spectroscopy analysis of the adduct of cyanuric acid and metaphosphoric acid. *Proceedings of the International Scientific-Practical Conference "Problems of Chemical Science, Its Application in Industry and Green Technologies"*, 680–682.

[19] Mardonov, U.M., Aslonova, F.S., Kholikova, G.K. (2026). Study of the reaction products of cyanuric acid with meta- and orthophosphoric acids by infrared spectroscopy. *Universum: Chemistry and Biology, 1*(139), 65–69.

[20] Frisch M.J., Schlegel H.B., Scuseria G.E., Robb M.A., Cheeseman J.R., Scalmani G., Fox D.J. (2019). Gaussian 16, Revision C.01. Gaussian, Inc., Wallingford CT.

[21] Becke, A. D. (1993). Density-functional thermochemistry. III. The role of exact exchange. The *Journal of Chemical Physics, 98*(7), 5648–5652.

[22] Lee, C., Yang, W., Parr, R.G. (1988). Development of the Colle-Salvetti correlation-energy formula into a functional of the electron density. *Physical Review B, 37*(2), 785–789.

[23] Binkley, J. S., Pople, J. A., Hehre, W. J. (1980). Self-consistent molecular orbital methods. 21. Small split-valence basis sets for first-row elements. *Journal of the American Chemical Society, 102*(3), 939–947.

[24] Chemcraft 1.8 (2015). Molecular visualization program. http://www.chemcraftprog.com

[25] Thompson, M.A., Glendening, E.D. (2004). ArgusLab docking engine. Planaria Software LLC. http://www.arguslab.com

[26] Chakraborty, S., Ray, S., Banerjee, S. (2024). Drug Repurposing in Quest for Newer Therapeutic Options Against Cancer. *Computational Biology in Drug Discovery and Repurposing*, 251–322.

[27] Šmydke, J. (2023). Using Koopmans' theorem for constructing basis sets: approaching high Rydberg excited states of lithium with a compact Gaussian basis. *Physical Chemistry Chemical Physics, 25*(30), 20250–20258. https://doi.org/10.1039/D2CP04633D

[28] Parr, R.G., Yang, W. (1989). *Density-Functional Theory of Atoms and Molecules*. Oxford University Press, New York.

[29] Parr, R.G., Szentpály, L.V., Liu, S. (1999). Electrophilicity index. *Journal of the American Chemical Society, 121*(9), 1922–1924.

[30] Yu, J., Yang, W. (2024). Chemical concepts from molecular orbital theory. *Exploring Chemical Concepts Through Theory and Computation*, 1–22.

[31] Jeffrey, G.A. (1997). *An Introduction to Hydrogen Bonding*. Oxford University Press, New York.

[32] Steiner, T. (2002). The hydrogen bond in the solid state. *Angewandte Chemie International Edition, 41*(1), 48–76.

[33] Taga, T., Sato, T., Kobayashi, M. (2008). Hydrogen-bonded structures in molecular crystals. *Journal of Molecular Structure, 875*(1–3), 102–110.

[34] Souto, M., Strutyński, K., Melle-Franco, M., Rocha, J. (2020). Electroactive organic building blocks for the chemical design of functional porous frameworks (MOFs and COFs) in electronics. *Chemistry–A European Journal, 26*(48), 10912–10935. https://doi.org/10.1002/chem.202001211

[35] Nishikiori, H., Kobayashi, M., Fujii, T. (2014). Hydrogen-bonding and vibrational features of molecular complexes. *Vibrational Spectroscopy, 70*, 68–74.

[36] Silverstein, R.M., Webster, F.X., Kiemle, D.J., Bryce, D.L. (2014). *Spectrometric Identification of Organic Compounds* (8th ed.). Wiley, Hoboken.

[37] Amaral, L. Q. D. (2021). Supramolecular Aggregates: Hardness Plus Softness. *Molecules, 26*(14), 4233. https://doi.org/10.3390/molecules26144233

[38] Chermette, H. (1999). Chemical reactivity indexes in density functional theory. *Journal of Computational Chemistry, 20*(1), 129–154.

[39] Gilli, G., Gilli, P. (2000). Towards an unified hydrogen-bond theory. *Journal of Molecular Structure, 552*(1–3), 1–15.

[40] Zulkefeli, M., Suzuki, A., Shiro, M., Hisamatsu, Y., Kimura, E., & Aoki, S. (2011). Selective hydrolysis of a phosphate monoester by a supramolecular phosphatase formed by self-assembly of a bis(Zn^{2+}-cyclen) complex, cyanuric acid, and copper. *Inorganic Chemistry, 50*(20), 10113–10123.

[41] Corbridge, D.E.C. (2013). *Phosphorus: Chemistry, Biochemistry and Technology* (6th ed.). CRC Press, Boca Raton.

[42] Sherrill, C.D. (2013). Energy component analysis of π interactions. *Accounts of Chemical Research, 46*(4), 1020–1028.

[43] Grabowski, S.J. (2011). What is the covalency of hydrogen bonding? *Chemical Reviews, 111*(4), 2597–2625.

[44] Scott, A.P., Radom, L. (1996). Harmonic vibrational frequencies: an evaluation of Hartree-Fock, Møller-Plesset, quadratic configuration interaction, density functional theory, and semiempirical scale factors. *The Journal of Physical Chemistry, 100*(41), 16502–16513.

[45] Merrick, J.P., Moran, D., Radom, L. (2007). An evaluation of harmonic vibrational frequency scale factors. *The Journal of Physical Chemistry A, 111*(45), 11683–11700.

[46] Kholikova, G.K., Mardonov, U.M., Ganiyev, B.Sh., Khazratova, D.A., Aliyeva, S.H., & Sharipov, M.S. (2025). Flame-retardant behavior of urea–metaphosphoric acid complexes on cellulose-based materials. *Journal of Chemistry and Technologies, 33*(4), 1136–1148. https://doi.org/10.15421/jchemtech.v33i4.336986